

Observation of \mathcal{PT} -symmetric quantum coherence in a single ion system

Wei-Chen Wang

Department of Physics, College of Liberal Arts and Sciences, National University of Defense Technology, Changsha 410073, China
Interdisciplinary Center for Quantum Information, National University of Defense Technology, Changsha 410073, China
These authors contributed equally to this work.

Yan-Li Zhou

Department of Physics, College of Liberal Arts and Sciences, National University of Defense Technology, Changsha 410073, China
Interdisciplinary Center for Quantum Information, National University of Defense Technology, Changsha 410073, China
These authors contributed equally to this work.

Hui-Lai Zhang

Key Laboratory of Low-Dimensional Quantum Structures and Quantum Control of Ministry of Education, and Department of Physics, Hunan Normal University, Changsha 410081, China

Jie Zhang

Department of Physics, College of Liberal Arts and Sciences, National University of Defense Technology, Changsha 410073, China
Interdisciplinary Center for Quantum Information, National University of Defense Technology, Changsha 410073, China

Man-Chao Zhang

Department of Physics, College of Liberal Arts and Sciences, National University of Defense Technology, Changsha 410073, China
Interdisciplinary Center for Quantum Information, National University of Defense Technology, Changsha 410073, China

Yi Xie

Department of Physics, College of Liberal Arts and Sciences, National University of Defense Technology, Changsha 410073, China
Interdisciplinary Center for Quantum Information, National University of Defense Technology, Changsha 410073, China

Chun-Wang Wu

Department of Physics, College of Liberal Arts and Sciences, National University of Defense Technology, Changsha 410073, China

Interdisciplinary Center for Quantum Information, National University of Defense Technology, Changsha 410073, China

Ting Chen

Department of Physics, College of Liberal Arts and Sciences, National University of Defense Technology, Changsha 410073, China

Interdisciplinary Center for Quantum Information, National University of Defense Technology, Changsha 410073, China

Bao-Quan Ou

Department of Physics, College of Liberal Arts and Sciences, National University of Defense Technology, Changsha 410073, China

Interdisciplinary Center for Quantum Information, National University of Defense Technology, Changsha 410073, China

Wei Wu

Department of Physics, College of Liberal Arts and Sciences, National University of Defense Technology, Changsha 410073, China

Interdisciplinary Center for Quantum Information, National University of Defense Technology, Changsha 410073, China

Hui Jing

Key Laboratory of Low-Dimensional Quantum Structures and Quantum Control of Ministry of Education, and Department of Physics, Hunan Normal University, Changsha 410081, China

E-mail: jinghui73@foxmail.com

Ping-Xing Chen

Department of Physics, College of Liberal Arts and Sciences, National University of Defense Technology, Changsha 410073, China

Interdisciplinary Center for Quantum Information, National University of Defense Technology, Changsha 410073, China

E-mail: pxchen@nudt.edu.cn

Abstract. Parity-time(\mathcal{PT})-symmetric physics, featuring real eigenvalues despite its non-Hermitian nature, has been demonstrated in diverse fields. \mathcal{PT} devices with unconventional functionalities, such as \mathcal{PT} -enhanced lasers or sensors, when approaching the exceptional point (EP) or the coalescences of both eigenvalues and eigenstates, have been realized mainly in the classical realm. In the quantum realm, the emergence of EP and its exotic effects have been observed in a microwave circuit, a solid-state device, and purely optical systems. Here, hidden \mathcal{PT} symmetry in a trapped cold $^{40}\text{Ca}^+$ ion is uncovered, with clear signatures of the transition from \mathcal{PT} -symmetric regime to \mathcal{PT} -broken regime. More importantly, a counterintuitive effect of perfect quantum coherence at the EP is observed in such a single-ion system. We

observed excellent agreement between experimental results and theoretical results. In view of the versatile role of cold ions in building quantum processors or sensors, our work provides a powerful new route to make and operate quantum EP devices at single-particle level.

1. Introduction

In conventional quantum mechanics, Hermiticity as a fundamental axiom ensures that physical observables have real eigenvalues [1]. A striking discovery in recent years has revealed parity-time(\mathcal{PT})-symmetric Hamiltonians [2, 3, 4], despite of their non-Hermitian nature, can also have real eigenvalues [5, 6]. In particular, by continuously tuning the parameter values, spontaneous breaking of \mathcal{PT} symmetry can take place at an exceptional point (EP) [7], where both the eigenvalues and the eigenstates of the system coalesce. As a result, many counterintuitive phenomena [8, 9, 10, 11, 12, 13, 14] emerge in such systems, e.g., single-mode lasing or anti-lasing [15, 16], loss-induced transparency or lasing [17, 18], EP-enhanced sensing [19, 20], to name only a few. These seminal experiments, however, have been performed mainly in the classical realm.

Achieving \mathcal{PT} symmetry, in principle, requires an exact gain-loss balance, which is challenging in quantum realm, since the system tends to be unstable due to noises amplified by the active gain [21]. To overcome this obstacle, one can construct an effective \mathcal{PT} -symmetric subsystem by coupling a Hermitian system to a dissipative reservoir [17, 18]. The emergence of EPs in such passive \mathcal{PT} systems, without any gain, has been demonstrated in experiments using purely optical elements [22] or solid-state devices [23, 24]. In particular, quantum coherence protection at EP was observed for a \mathcal{PT} -broken superconducting circuit [23], in which one of the three energy levels of a transmon circuit was treated as an effective reservoir to obtain a \mathcal{PT} -symmetric two-level system [23]. While the results were post-selected and the success rate decreased exponentially for longer times, that experiment opened up a practical route to explore truly quantum EP effects, for applications in emerging non-Hermitian quantum technologies.

Here we demonstrate that \mathcal{PT} symmetry and its spontaneous breaking can be achieved and well controlled in a single-ion device, by using two internal states of $^{40}\text{Ca}^+$ ion, together with an ancillary state of the same ion simulating the lossy environment. We note that as a promising candidate for building quantum information processing, trapped cold ions having a coherence time as long as 10 minutes [25] have been widely used for quantum memory [26, 27, 28], quantum state preparation [29], quantum simulation [30, 31, 32, 33] and high-precision metrology [34, 35]. However, up to date, experimental realization of \mathcal{PT} symmetry in a trapped ion system has not been achieved, hindering its applications in non-Hermitian quantum control of ions. Here we fill this gap by demonstrating clear signatures of quantum EP in a $^{40}\text{Ca}^+$ ion. We deterministically demonstrate EP features by measuring the ion-state populations both in the \mathcal{PT} -symmetric (PTS) regime and in the \mathcal{PT} -broken (PTB) regime. More importantly, by approaching the EP, a tuning point is observed in non-diagonal elements of the density matrix, at which giant enhancement of quantum coherence [36] can be achieved for the system. Our work is the first step towards exploring non-Hermitian quantum effects at single-ion level, for applications towards e.g., building quantum processors or sensors with \mathcal{PT} -symmetric cold ions.

2. RESULTS

2.1. Experimental platform: passive \mathcal{PT} -symmetry in a single ion

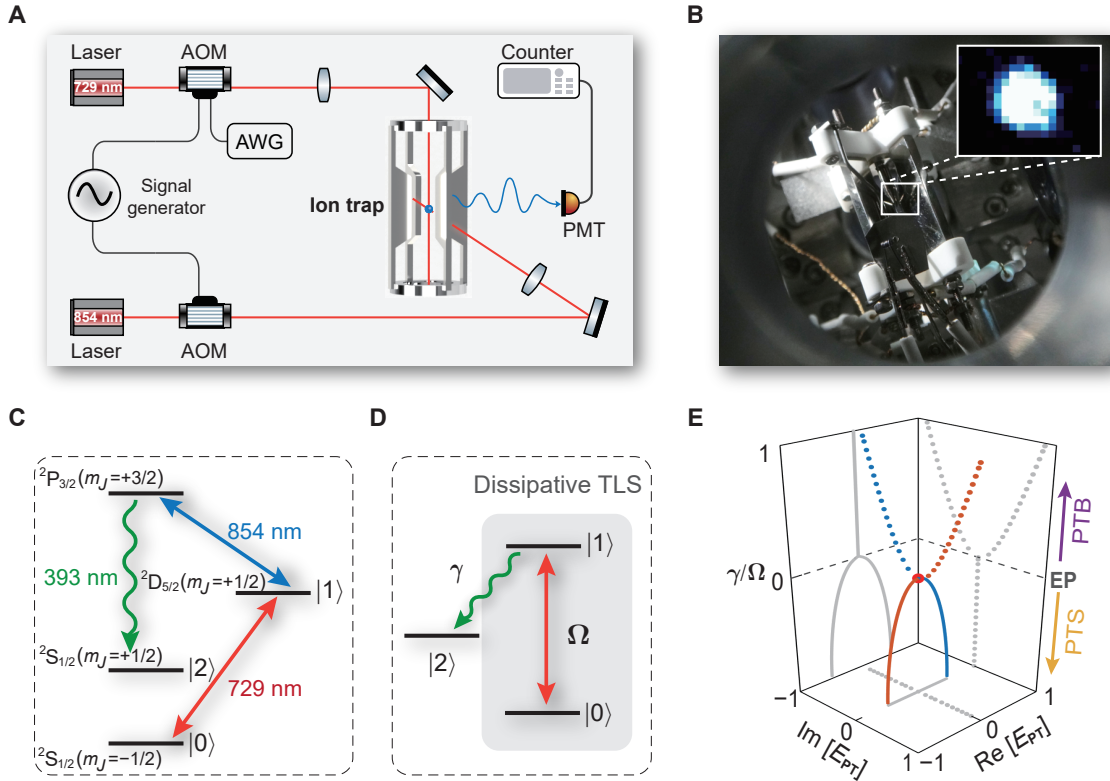


Figure 1: **The passive \mathcal{PT} -symmetric single-ion system.** (A) Schematic diagram of the experimental device. During the experiment, both 729 nm and 854 nm laser beams are switched on at the same time, and the quantum states of the ion at different times are read out by the electron shelving. (AOM: acousto-optical modulators. PMT: photomultiplier tube. AWG: arbitrary waveform generator). (B) The photograph of the ion trap. (C-D) The energy levels of the $^{40}\text{Ca}^+$ ion, with the internal states $|0\rangle$, $|1\rangle$ and $|2\rangle$ corresponding to the energy levels $^2\text{S}_{1/2}(m_J = -1/2)$, $^2\text{D}_{5/2}(m_J = +1/2)$ and $^2\text{S}_{1/2}(m_J = +1/2)$, respectively. (E) The eigenvalues of $H_{\mathcal{PT}}$ versus γ/Ω . The projection on the back (dotted lines) and the left (thick lines) show the evolution of the imaginary parts and real parts, respectively. The projection on the bottom shows the evolution of the eigenfrequencies in the complex plane. EP is corresponding to $\gamma = \Omega$.

In our experiment, we used a single trapped $^{40}\text{Ca}^+$ ion to realize the passive \mathcal{PT} -symmetry. The experimental setup and the energy levels of the $^{40}\text{Ca}^+$ are depicted in Fig. 1A-C. The ion was initially prepared in the ground state $|0\rangle = |^2\text{S}_{1/2}(m_J = -1/2)\rangle$ and was driven to the excited state $|1\rangle = |^2\text{D}_{5/2}(m_J = +1/2)\rangle$ by a laser with wavelength 729 nm. To induce a tunable loss γ in $|1\rangle$, we used a laser beam at 854 nm to couple $|1\rangle \leftrightarrow |^2\text{P}_{3/2}(m_J = +3/2)\rangle$, which is a short-life level and decays quickly to the

state $|2\rangle = |^2\text{S}_{1/2}(m_J = +1/2)\rangle$. With this configuration, the system exhibits coherent transitions between $|0\rangle$ and $|1\rangle$ with $|1\rangle$ experiencing loss (Fig. 1D). This two-level system in the presence of coherent transition and loss can be described by an effective non-Hermitian Hamiltonian (see Supplemental notes 1)

$$H_{\text{eff}} = \frac{\Omega}{2}\sigma_x - i\gamma|1\rangle\langle 1| = H_{\mathcal{PT}} - i\frac{\gamma}{2}\mathbf{I}, \quad (1)$$

where $H_{\mathcal{PT}} = \frac{\Omega}{2}\sigma_x - i\frac{\gamma}{2}\sigma_z$ is \mathcal{PT} -symmetric Hamiltonian and $\sigma_{x(z)}$ is the Pauli matrix and \mathbf{I} is the identity operator.

This \mathcal{PT} -symmetric system consists of a bipartite system with balanced gain and loss. The central feature of \mathcal{PT} -symmetric system is a transition from broken to unbroken \mathcal{PT} -symmetry, which is governed by the interplay of the gain-loss rate ($\gamma/2$) and the mutual coupling rate $\Omega/2$. As shown in Fig. 1E, when the gain-loss rate is smaller than the coupling rate between the two state ($\gamma/\Omega < 1$), the system exhibits a real spectrum and simultaneous eigenmodes of the Hamiltonian associated with oscillatory solutions. This region is referred to as PTS phase. Yet when the gain-loss rate is bigger than the coupling rate ($\gamma/\Omega > 1$), we call it PTB phase where complex conjugate eigenvalues emerge, and one of the eigenmodes exponentially grows [See Supplemental Notes 1]. The transition between the PTS and PTB phases takes place at an exceptional point (EP) which emerges for $\gamma = \Omega$. The behavior of the eigenvalues of a \mathcal{PT} -symmetric system is shown in Fig. 1E, highlighting the bifurcation associated with the spontaneous symmetry breaking at the EP [7].

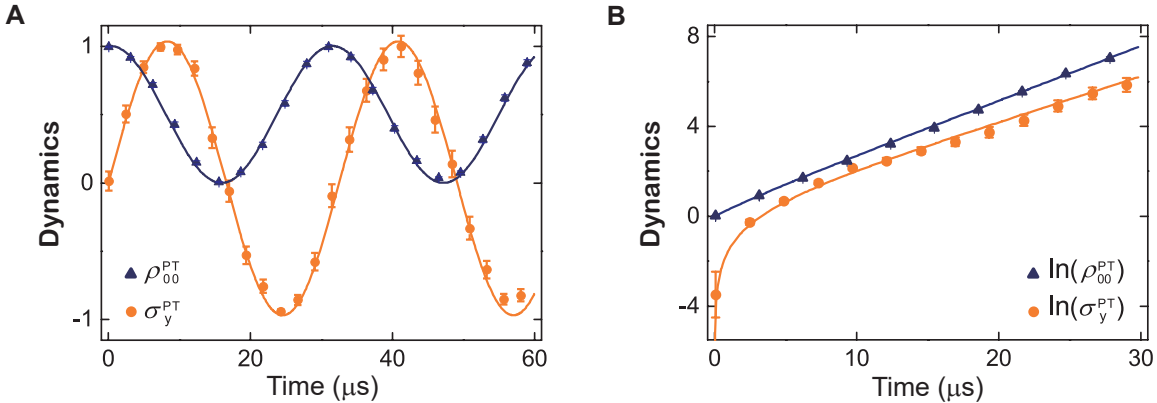


Figure 2: Dynamical evolution of the \mathcal{PT} -symmetric system in the initial state $|0\rangle$ in the PTS phase (A) and PTB phase (B), respectively. (A) $\Omega = 2\pi \times 32$ (kHz), $\gamma = 2\pi \times 1$ (kHz), (B) $\Omega = 2\pi \times 32$ (kHz), $\gamma = 2\pi \times 47$ (kHz). The marks represent experimental data, and the lines represent theoretical fit. The error bars are the standard deviation of the measurements.

Now we investigate these predictions in our experiments. We first verify the dynamical behaviors of the \mathcal{PT} -symmetric system at different phases. We initialize the system in the state $|0\rangle$ and tune the coupling $\Omega = 2\pi \times 32$ (kHz) at time $t = 0$. The loss rate is tuning to different values. We characterize the \mathcal{PT} symmetry-breaking

transitions using the observed experimental signatures in the populations of $|0\rangle$ and the coherences in the $\{|0\rangle, |1\rangle\}$ qubit manifold, which have the following forms [see Supplemental notes 1]:

$$\rho_{00}^{\mathcal{PT}}(t) = [-\Omega^2 + (2\gamma^2 - \Omega^2) \cosh(\kappa t) + 2\gamma\kappa \sinh(\kappa t)]/2\kappa^2, \quad (2)$$

$$\langle \sigma_y^{\mathcal{PT}}(t) \rangle = \text{Tr}[\sigma_y \rho^{\mathcal{PT}}] = \Omega [-\gamma + \gamma \cosh(\kappa t) + \kappa \sinh(\kappa t)]/\kappa^2, \quad (3)$$

with $\kappa = \sqrt{\gamma^2 - \Omega^2}$. We see that when $\gamma > \Omega$, κ is real and the system evolves as $e^{-\kappa t}$ and $e^{\kappa t}$. But when $\gamma < \Omega$, $\sinh(\kappa t)(\cosh(\kappa t))$ corresponds to time evolution $e^{\pm i|\kappa|t}$, which results in the oscillatory evolution at angular frequency $|\kappa|$.

The experiment results are shown in Figs. 2A, B. When γ/Ω is tuned to the PTS phase, the population and the coherence exhibits oscillation with frequency $|\kappa|$. In contrast, when γ/Ω is tuned to the PTB phase, both of the population ($\rho_{00}^{\mathcal{PT}}$) and the coherence ($\langle \sigma_y^{\mathcal{PT}}(t) \rangle$) increase exponentially. All the experimental results agree with the theoretical phase diagram very well. This means \mathcal{PT} -symmetry-breaking transitions can be probed in this system just by controlling loss rate γ , which can be tuned by varying the power of a laser beam (see Supplemental notes 2).

2.2. \mathcal{PT} phase transition in the experimental system

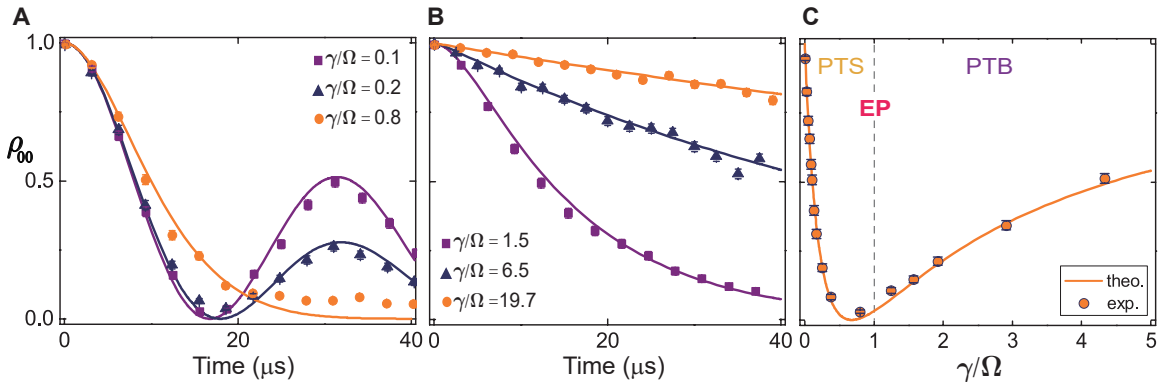


Figure 3: (A-B) Dynamical evolution of experimental system in the initial state $|0\rangle$. Coupling strength Ω is about $2\pi \times 32$ (kHz). (A) In the PTS phase, the amplitude of population of $|0\rangle$ decreases faster with the increase of ratio $\gamma/\Omega = 0.1$ (Purple line), 0.2 (Navy blue line), 0.8 (Orange line). (B) In the PTB phase, with the increase of ratio $\gamma/\Omega = 1.5$ (Purple line), 6.5 (Navy blue line), 19.7 (Orange line), the population of state $|0\rangle$ is suppressed. (C) The population of the state $|0\rangle$ versus the loss rate γ . Loss-induced suppression and revival of the population of the state $|0\rangle$ when increasing γ in the vicinity of EP can be clearly seen. The circles are the experimental data measured at a fixed time $t = 2\pi/\Omega$ with $\Omega = 2\pi \times 32$ (kHz), while the line is from the theoretical fit. The error bars are the standard deviation of the measurements.

In this system, EP may also emerge when a loss imbalance is achieved, as described by H_{eff} (see Fig. S1 in Supplemental notes 1). The dynamical relationship between

the experimental system and the simulated \mathcal{PT} -symmetric system is $\rho(t) = e^{-\gamma t} \rho_{\mathcal{PT}}(t)$. The experimental system in the PTS phase will decay while oscillating (Fig. 3A) and eventually evolve to the ground state of the system. Meanwhile, the oscillation period gradually becomes infinite as $\gamma \rightarrow \Omega$. But in the PTB phase, it will monotonically decay into the stationary state (Fig. 3B).

Figs. 3A, B also show that, in the PTS phase, the population of $|0\rangle$ in the experiment system decreases when the loss increases. On the contrary, in the PTB phase, the population of $|0\rangle$ increases when the loss increases. In order to show more intuitively about this phenomenon, we studied how the population of $|0\rangle$ in the experimental system changes with γ/Ω at a fixed time. We measured the population of $|0\rangle$ at different loss rates at time $t = 2\pi/\Omega$ with $\Omega = 2\pi \times 32$ (kHz). The results are shown in Fig. 3C. We observe that a turning point emerges for the population of the state $|0\rangle$, which can be well explained by considering the EP of the H_{eff} : When the loss rate $\gamma = 0$, the population of the two states $|0\rangle$ and $|1\rangle$ can be freely exchanged with each other. By increasing the loss rate ($\gamma < \Omega$), the population of level $|1\rangle$ will decay to $|2\rangle$ while oscillating and hence the population of the state $|0\rangle$ will also decrease while oscillating. At the EP ($\gamma = \Omega$), the coherent coupling balances with the loss of $|1\rangle$ state, the population of $|0\rangle$ state reaches stable states. After this point ($\gamma > \Omega$), as the loss increased, the $|0\rangle$ state will become localized, since the loss is so strong that the transition from $|0\rangle$ to $|1\rangle$ state can be neglected. This behavior is a manifestation of the progressive localization of two energy levels with unequal loss.

The observed phenomenon is similar to the loss-induced lasing reported in a classical system [18]. Note that, the lowest point γ_{min} in Fig. 3C is not the EP. The explanation is that the system is not at the final stationary state when we do the measurement at time $t = 2\pi/\Omega$. Generally, when processing experimental data, we selected the population number at a fixed time. As a result, the loss γ_{min} in Fig. 3C is slightly different from EP. If we set the time long enough, the lowest point will be closer to the EP.

2.3. Quantum coherence at the EP

In our experiment, \mathcal{PT} -symmetry-breaking transitions at the EP corresponds to the phase transition of a quantum system. To visualize the effect of the phase transition at the EP further, we introduce the order parameter by the time average of $\langle \sigma_z \rangle$ defined in [37]

$$\Sigma_Z(\gamma) = \lim_{T \rightarrow \infty} \frac{1}{T} \int_0^T \frac{\langle \sigma_z(\gamma, t) \rangle}{\text{Tr}[\rho(\gamma, t)]} dt = \begin{cases} 0, & 0 < \gamma < \Omega, \\ -\sqrt{\gamma^2 - \Omega^2}/\gamma, & \gamma \geq \Omega. \end{cases} \quad (4)$$

Meanwhile, to investigate the features of quantum coherent in the vicinity of EP, we introduce the another order parameter by the time average of $\langle \sigma_y \rangle$

$$\Sigma_Y(\gamma) = \lim_{T \rightarrow \infty} \frac{1}{T} \int_0^T \left| \frac{\langle \sigma_y(\gamma, t) \rangle}{\text{Tr}[\rho(\gamma, t)]} \right| dt = \begin{cases} \Omega [\pi - 2 \arccos(\gamma/\Omega)] / (\gamma\pi), & 0 < \gamma < \Omega, \\ \Omega/\gamma, & \gamma \geq \Omega, \end{cases} \quad (5)$$

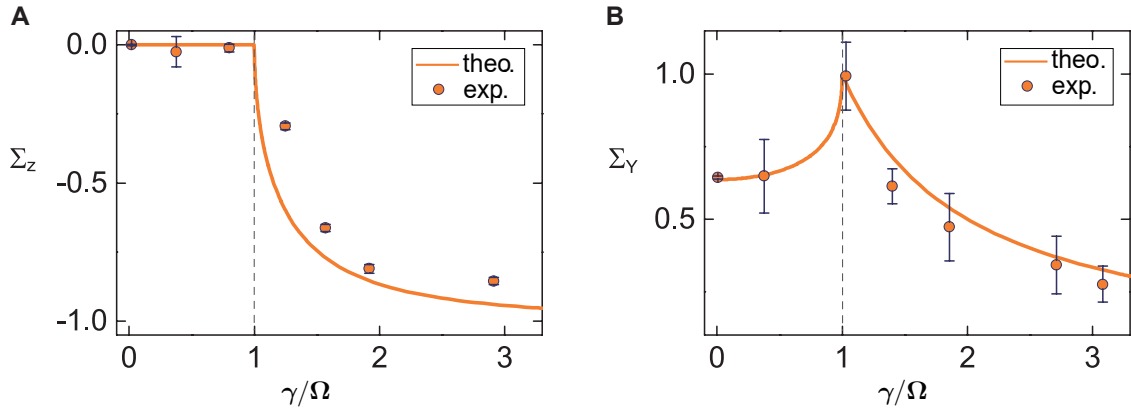


Figure 4: **A(B):** The order parameters $\Sigma_{Z(Y)}$ versus γ with the initial state $|0\rangle$ and $\Omega = 2\pi \times 32$ (kHz). The error bars indicate the estimated error from the fit to the dynamical equation $\rho(t)$.

where $|\cdot|$ is the abstract value. We have to mention that both $\rho(t)$ and $\rho_{\mathcal{PT}}(t)$, on their own, do not preserve the trace of the density operator (see Supplemental notes 1 and Fig. S3). For $\rho(t)$, which is associated with a dissipative system, the trace decays regardless of whether the system is in PTS or PTB phase. But for $\rho_{\mathcal{PT}}(t)$, which has loss and gain, the trace exhibits \mathcal{PT} symmetric phase transition phenomenon. So if we want to know the relative dynamics of the system, we need to renormalize $\rho(t)(\rho_{\mathcal{PT}}(t))$ dividing them to their traces. After renormalization, the dynamical behaviors of $\rho(t)$ and $\rho_{\mathcal{PT}}(t)$ are the same.

The order parameters Σ_Z and Σ_Y given in Eqs. 4 and 5 are not dependent on the initial state, and they are determined just by the ratio γ/Ω . Moreover, they both reveal the phase transition at the EP ($\gamma = \Omega$). Eqs. 4 and 5 also tell us that at the EP, the populations of $|0\rangle$ and $|1\rangle$ are equally, and the system is in a long-lived coherent superposition of $|0\rangle$ and $|1\rangle$ (see Supplemental notes 1).

The order parameter Σ_Z reveals the energy of the \mathcal{PT} -symmetric system along with the change of γ . The experimental results are shown in Fig. 4A. In the PTS phase, because the system oscillates periodically, average populations of $|0\rangle$ and $|1\rangle$ states are the same, which results in Σ_Z zero. While in the PTB phase, the system will finally evolve to the stationary state, in which the population of the system will be bound to state $|0\rangle$ and unable to transit to state $|1\rangle$ with the increase of γ . However, Σ_Z can only show the systemic energy, so the similar phenomenon can also be obtained in the classical \mathcal{PT} -symmetric system. In order to reflect the characteristics of the quantum \mathcal{PT} -symmetric system, we must show the quantum properties near the EP. Comparing with previous quantum experiments which are used for simulating \mathcal{PT} -symmetric system [24, 38], we further investigated the quantum coherence Σ_Y of the \mathcal{PT} -symmetric systems (Fig. 4B). We observed that the quantum coherence of \mathcal{PT} -symmetric system near the EP reaches the maximum value, and the EP significantly enhance the quantum coherence of the system. This is because in the EP, the gain and

loss of the system balances the rate of coherent transitions so that the system achieves a stable state, which is the coherent superposition of $|0\rangle$ and $|1\rangle$ at EP(see Supplemental notes 1).

Considering that the imaginary part of the coherence is the embodiment of absorptive capacity of the \mathcal{PT} -symmetric system, we could say that at the EP the transition rate between $|0\rangle \leftrightarrow |1\rangle$ is the largest, which may be applicable in quantum engineer, such as increasing the rate of ion cooling. We note that recently in a warm atomic system [39], the enhancement of quantum discord has been shown in the anti- \mathcal{PT} -symmetry unbroken phase by engineering the dissipative coupling between two optical channels. Our experiment along with the results in [39], imply obviously the coherence enhance in EP.

3. Conclusion

In summary, we have demonstrated \mathcal{PT} symmetry and its spontaneous breaking in a single $^{40}\text{Ca}^+$ ion system. When the system is steered to an EP and past it, both the mean populations of the ion states and the quantum coherence exhibit a turning point. To the best of our knowledge, this is the first work on experimental observation of \mathcal{PT} symmetry in a single trapped ion, revealing the counterintuitive EP-enabled effect of enhanced quantum coherence. In view of the ultra-long coherence time of trapped ions, together with well developed techniques of engineering their quantum states, our work provides a powerful new tool for exploring and utilizing truly quantum EP effects at single-ion levels. In a broader view, our work can also help to design and utilize unconventional ion-based devices, such as non-Hermitian quantum memory, quantum simulators, or quantum sensors.

- [1] C. M. Bender, S. Boettcher, Real Spectra in Non-Hermitian Hamiltonians Having \mathcal{PT} Symmetry. *Phys. Rev. Lett.* **80**, 5243 (1998).
- [2] Y. Ashida, Z. Gong, and M. Ueda, Non-Hermitian Physics, *arXiv:2006.01837* [cond-mat, physics:quant-ph] (2020).
- [3] R. El-Ganainy, K. G. Makris, M. Khajavikhan, Z. H. Musslimani, S. Rotter, and D. N. Christodoulides, Non-Hermitian physics and PT symmetry, *Nat. Phys.* **14**, 11 (2018).
- [4] S. K. Özdemir, S. Rotter, F. Nori, and L. Yang, Paritytime symmetry and exceptional points in photonics. *Nat. Mater.* **18**, 783 (2019).
- [5] C. M. Bender, D. C. Brody, H. F. Jones, Complex Extension of Quantum Mechanics. *Phys. Rev. Lett.* **89**, 270401 (2002).
- [6] C. M. Bender, Making sense of non-Hermitian Hamiltonians. *Rept. Prog. Phys.* **70**, 947 (2007).
- [7] M.-A. Miri, A. Alù, Exceptional points in optics and photonics. *Science* **363**, 42 (2019).
- [8] R. El-Ganainy ,K. G. Makris, M. Khajavikhan, Z. H. Musslimani, S. Rotter, D. N. Christodoulides, Non-Hermitian physics and PT symmetry. *Nat. Phys.* **14**, 11-19 (2018).
- [9] Y. C. Lee, M. H. Hsieh, S. T. Flammia, R. K. Lee, Local PT Symmetry Violates the No-Signaling Principle. *Phy. Rev. Lett.* **112**, 130404 (2014).
- [10] H. Jing, S. K. Oezdemir , X. Y. Lue, PT-Symmetric Phonon Laser. *Phy. Rev. Lett.* **113**, 053604 (2014).
- [11] C. M. Bender , D. C. Brody, H. F. Jones, Meister, B. K, Faster than Hermitian Quantum Mechanics. *Phys. Rev. Lett.* **98**, 040403 (2007).

- [12] U. Günther, B. F. Samsonov, Naimark-Dilated PT-Symmetric Brachistochrone. *Phys. Rev. Lett.* **101**, 230404 (2008).
- [13] R. El-Ganainy, K. G. Makris, D. N. Christodoulides, Z. H. Musslimani, Theory of coupled optical PT-symmetric structures. *Opt. Lett.* **32**, 2632-2634 (2007).
- [14] S. Klaiman, U. Günther, N. Moiseyev, Visualization of Branch Points in PT-Symmetric Waveguides. *Phys. Rev. Lett.* **101**, 080402 (2008).
- [15] L. Feng, Z. J. Wong, R.-M. Ma, Y. Wang, and X. Zhang, Single-mode laser by parity-time symmetry breaking. *Science* **346**, 972 (2014).
- [16] H. Hodaei, M.-A. Miri, M. Heinrich, D. N. Christodoulides, M. Khajavikhan, Parity-time-symmetric microring lasers. *Science* **346**, 975 (2014).
- [17] B. Peng, S. K. zdemir, S. Rotter, H. Yilmaz, M. Liertzer, F. Monifi, C. M. Bender, F. Nori, L. Yang, Loss-induced suppression and revival of lasing, *Science* **346**, 328 (2014).
- [18] A. Guo, G. J. Salamo, D. Duchesne, R. Morandotti, G. A. Siviloglou, D. N. Christodoulides, Observation of PT-Symmetry Breaking in Complex Optical Potentials. *Phys. Rev. Lett.* **103**, 093902 (2009).
- [19] W. Chen, S. K. zdemir, G. Zhao, J. Wiersig, and L. Yang, Exceptional points enhance sensing in an optical microcavity. *Nature* **548**, 192 (2017).
- [20] H. Hodaei, A. U. Hassan, S. Wittek, H. Garcia-Gracia, R. El-Ganainy, D. N. Christodoulides, and M. Khajavikhan, Enhanced sensitivity at higher-order exceptional points, *Nature* **548**, 187 (2017).
- [21] S. Scheel, A. Szameit, PT-symmetric photonic quantum systems with gain and loss do not exist. *Europhys. Lett.* **122**, 34001 (2018).
- [22] L. Xiao, X. Zhan, Z. H. Bian, K. K. Wang, X. Zhang, X. P. Wang, J. Li, K. Mochizuki, D. Kim, N. Kawakami, W. Yi, H. Obuse, B. C. Sanders, P. Xue, Observation of topological edge states in paritytime-symmetric quantum walks. *Nat. Phys.* **13**, 1117 (2017).
- [23] M. Naghiloo, M. Abbasi, Y. N. Joglekar, K. W. Murch, Quantum state tomography across the exceptional point in a single dissipative qubit, *Nat. Phys.* **15**, 1232 (2019).
- [24] Y. Wu, W. Q. J. P. Geng, X. R. Song, X. Y. Ye, XY, C. K. Duan, X. Rong, J. F. Du, Observation of parity-time symmetry breaking in a single-spin system. *Science* **364**, 878-880 (2019).
- [25] Y. Wang, M. Um, J. H. Zhang, S. M. An, M. Lyu, J. N. Zhang, L. M. Duan, D. Yum, K. Kim, Single-qubit quantum memory exceeding ten-minute coherence time. *Nat. Photon.* **11**, 646-650 (2017).
- [26] B. Tabakov, J. Bell, D. F. Bogorin, B. Bonenfant, P. Cook, L. Disney, T. Dolezal, J. P. O'Reilly, J. Phillips, K. Poole, L. Wessing, K. A. Brickman-Soderberg, Towards using trapped ions as memory nodes in a photon-mediated quantum network. *Proceedings of SPIE*, **10660**, 1-7 (2018).
- [27] D. Kielpinski; V. Meyer; M. A. Rowe; C. A. Sackett; W. M. Itano; C. Monroe; D. J. Wineland, A Decoherence-Free Quantum Memory Using Trapped Ions. *Science* **291**, 1013-1015 (2001).
- [28] C. Monroe, R. Christopher, D. J. Wineland, Quantum computing with ions. *Scientific American* **299**, 64-71 (2008).
- [29] T. Brydges, A. Elben, P. Jurcevic, B. Vermersch, C. Maier, B. P. Lanyon, P. Zoller, R. Blatt, C. F. Roos, Probing Rényi entanglement entropy via randomized measurements. *Science* **364**, 260-263 (2019).
- [30] J. Zhang, G. Pagano, P. W. Hess, A. Kyprianidis, P. Becker, H. Kaplan, A. V. Gorshkov, Z.-X. Gong, C. Monroe, Observation of a Many-Body Dynamical Phase Transition with a 53-Qubit Quantum Simulator. *Nature*, **551**, 601-604 (2017).
- [31] B. P. Lanyon, C. Hempel, D. Nigg, M. Müller, R. Gerritsma, F. Z?hringer, P. Schindler, J. T. Barreiro, M. Rambach, G. Kirchmair, M. Hennrich, P. Zoller, R. Blatt, C. F. Roos, Universal Digital Quantum Simulation with Trapped Ions. *Science*, **334**, 57-61 (2011).
- [32] R. Blatt, C. F. Roos, Quantum simulations with trapped ions. *Nat. Phys.* **8**, 277-284 (2012).
- [33] C. Schneider, D. Porras, T. Schaetz, Experimental quantum simulations of many-body physics with trapped ions. *Rep. Prog. Phys.* **75**, 024401 (2012).

- [34] T. Rosenband, D. B. Hume, P. O. Schmidt, C. W. Chou, A. Brusch, L. Lorini, W. H. Oskay, R. E. Drullinger, T. M. Fortier, J. E. Stalnaker, S. A. Diddams, W. C. Swann, N. R. Newbury, W. M. Itano, D. J. Wineland, J. C. Bergquist, Frequency Ratio of Al^+ and Hg^+ Single-Ion Optical Clocks; Metrology at the 17th Decimal Place. *Science*. **319**, 1808-1812 (2008).
- [35] N. Huntemann, M. Okhapkin, B. Lipphardt, S. Weyers, Chr. Tamm, and E. Peik, High-accuracy optical clock based on the octupole transition in $^{171}\text{Yb}^+$. *Phys. Rev. Lett.* **108**, 090801 (2012).
- [36] T. Baumgratz, M. Cramer, and M. B. Plenio, Quantifying Coherence. *Phys. Rev. Lett.* **113**, 140401 (2014).
- [37] D. C. Brody, E. M. Graefe, Mixed-State Evolution in the Presence of Gain and Loss. *Phys. Rev. Lett.* **109**, 230405 (2012).
- [38] J. M. Li, A. K. Harter, J. Liu, L. de Melo, Y. N. Joglekar, L. Luo, Observation of parity-time symmetry breaking transitions in a dissipative Floquet system of ultracold atoms. *Nat. Commun.* **10**, 855 (2019).
- [39] W. Cao, X. Lu, X. Meng, J. Sun, H. Shen, and Y. Xiao, Reservoir-Mediated Quantum Correlations in Non-Hermitian Optical System, *Phys. Rev. Lett.* **124**, 030401 (2020).

4. Acknowledgments

Funding: This work was supported by the National Basic Research Program of China under Grant No. 2016YFA0301903, the National Natural Science Foundation of China under Grant No. 61632021, No. 11935006, No. 11774086, No.11871472, the Natural Science Foundation of Hunan Province of China under Grant No. 2018JJ2467.

Author contributions: P.X.C. and H.J. conceived the project. W.C.W. and J.Z. performed the experiments and analyzed the data; Y.L.Z., C.W.W. and P.X.C. provided theory support. Y.L.Z., W.C.W., H.L.Z., H.J. and P.X.C. wrote the manuscript. All authors discussed the results and contributed to the manuscript.

Competing interests: The authors declare that they have no competing interests.

Data and materials availability: All data needed to evaluate the conclusions in the paper are present in the paper and/or the Supplementary Materials. Additional data related to this paper may be requested from the authors

Appendix A. Supplementary

Appendix A.1. S1: The analytical form of dynamics of the experimental system

This full system can be considered as a three-level system, where $|0\rangle \leftrightarrow |1\rangle$ transition is driven by the laser with Rabi frequency Ω , and the decay $|1\rangle \rightarrow |2\rangle$ corresponds to the loss of the system. The time evolution of the full system obeys a Lindblad master equation $\dot{\sigma}(t) = \mathfrak{L}\sigma$, where the generator of the dynamics \mathfrak{L} is normally called Liouvillian superoperator, and has the form

$$\mathfrak{L}(\cdot) := -i[H, (\cdot)] + (J(\cdot)J^\dagger - 2\{J^\dagger J, (\cdot)\}), \quad (\text{S1})$$

here σ is the density matrix of the three-level system, $H = \frac{\Omega}{2}(|0\rangle\langle 1| + |1\rangle\langle 0|)$ is the Hamiltonian and $J = \sqrt{\gamma}|2\rangle\langle 1|$ is the quantum jump operators, with γ the tunable decay rate.

From equation (S1), we get

$$\dot{\sigma}_{11} = -2\gamma\sigma_{11} - i\frac{\Omega}{2}(\sigma_{01} - \sigma_{10}), \quad (\text{S2a})$$

$$\dot{\sigma}_{00} = i\frac{\Omega}{2}(\sigma_{01} - \sigma_{10}), \quad (\text{S2b})$$

$$\dot{\sigma}_{01} = -\gamma\sigma_{01} + i\frac{\Omega}{2}(\sigma_{00} - \sigma_{11}). \quad (\text{S2c})$$

So the density matrix $\rho(t)$ for the subspace $\{|0\rangle, |1\rangle\}$ is determined by a lower dimension Liouvillian superoperator $\dot{\rho} = \mathcal{L}\rho(t)$ with

$$\mathcal{L} = \begin{pmatrix} -2\gamma & i\frac{\Omega}{2} & -i\frac{\Omega}{2} & 0 \\ i\frac{\Omega}{2} & -\gamma & 0 & -i\frac{\Omega}{2} \\ -i\frac{\Omega}{2} & 0 & -\gamma & i\frac{\Omega}{2} \\ 0 & -i\frac{\Omega}{2} & i\frac{\Omega}{2} & 0 \end{pmatrix}. \quad (\text{S3})$$

If we define an effective, non-Hermitian Hamiltonian by $H_{\text{eff}} = \Omega/2\sigma_x - i\gamma|1\rangle\langle 1|$, where σ_x is the Pauli matrix, we can rewrite Lindblad master equation like

$$\dot{\rho}(t) = \mathcal{L}\rho = -i[H_{\text{eff}}\rho - \rho H_{\text{eff}}^\dagger], \quad (\text{S4})$$

where we have introduced the Liouvillian superoperator \mathcal{L} without quantum jumps. This means that Liouvillian superoperator \mathcal{L} plays the same role with the non-Hermitian Hamiltonian. Since the Liouvillian \mathcal{L} is a non-Hermitian matrix, it too can exhibit EPs, which can be defined as the degeneracy points of \mathcal{L} [1].

We get the eigenvalues and eigenvectors of H_{eff} via the relation $H_{\text{eff}}|\phi_i\rangle = E_i|\phi\rangle$ [1]

$$\{E_{\text{eff}}\} = \frac{1}{2}\{-i\gamma + \sqrt{\Omega^2 - \gamma^2}, \frac{1}{2} - i\gamma - \sqrt{\Omega^2 - \gamma^2}\}, \quad (\text{S5a})$$

$$\{\phi\} \propto \left\{ \{-i\gamma + \sqrt{\Omega^2 - \gamma^2}, \Omega\}^\top, \{-i\gamma - \sqrt{\Omega^2 - \gamma^2}, \Omega\}^\top \right\}. \quad (\text{S5b})$$

In the same to diagonalize H_{eff} , one can obtain much information about the experimental system by find the eigenvalues of \mathcal{L} [1, 2]. The eigenvalues of \mathcal{L} are $\{\lambda_1 = -\gamma + \kappa, \lambda_{2(3)} = -\gamma, \lambda_4 = -\gamma - \kappa\}$ with $\kappa = \sqrt{\gamma^2 - \Omega^2}$ (which we order by decreasing real part, $\text{Re}[\lambda_i] \geq \text{Re}[\lambda_{i+1}]$). Every eigenvalue λ_i corresponds to a right eigenmatrix R_i and a left eigenmatrix L_i of \mathcal{L} , which are defined by $\mathcal{L}R_i = \lambda_i R_i$ and $\mathcal{L}^\dagger L_i = \lambda_i^* L_i$. The eigensystem of Liouvillian superoperator \mathcal{L} can be written as (not normalized)

$$\{\lambda\} = \{-\gamma + \kappa, -\gamma, -\gamma, -\gamma - \kappa\}, \quad (\text{S6a})$$

$$\{R\} = \left\{ \begin{pmatrix} -\frac{2\gamma(-\gamma+\kappa)+\Omega^2}{\Omega^2} & i\frac{(-\gamma+\kappa)}{\Omega} \\ -i\frac{(-\gamma+\kappa)}{\Omega} & 1 \end{pmatrix}, \begin{pmatrix} 1 & -i\frac{\gamma}{\Omega} \\ 0 & 1 \end{pmatrix}, \begin{pmatrix} 0 & 1 \\ 1 & 0 \end{pmatrix}, \begin{pmatrix} \frac{2\gamma(\gamma+\kappa)-\Omega^2}{\Omega^2} & -i\frac{(\gamma+\kappa)}{\Omega} \\ i\frac{(\gamma+\kappa)}{\Omega} & 1 \end{pmatrix} \right\}. \quad (\text{S6b})$$

We can see that the relation between the eigenvalues properties of \mathcal{L} and H_{eff} is $\lambda_i = -i(E_j - E_k^*)$ and the eigenmatrices of \mathcal{L} is given by $R_i = \{|\phi_j\rangle\langle\phi_k|\}$. Therefore, the EP of H_{eff} is obviously the same with \mathcal{L} (see Fig. S1).

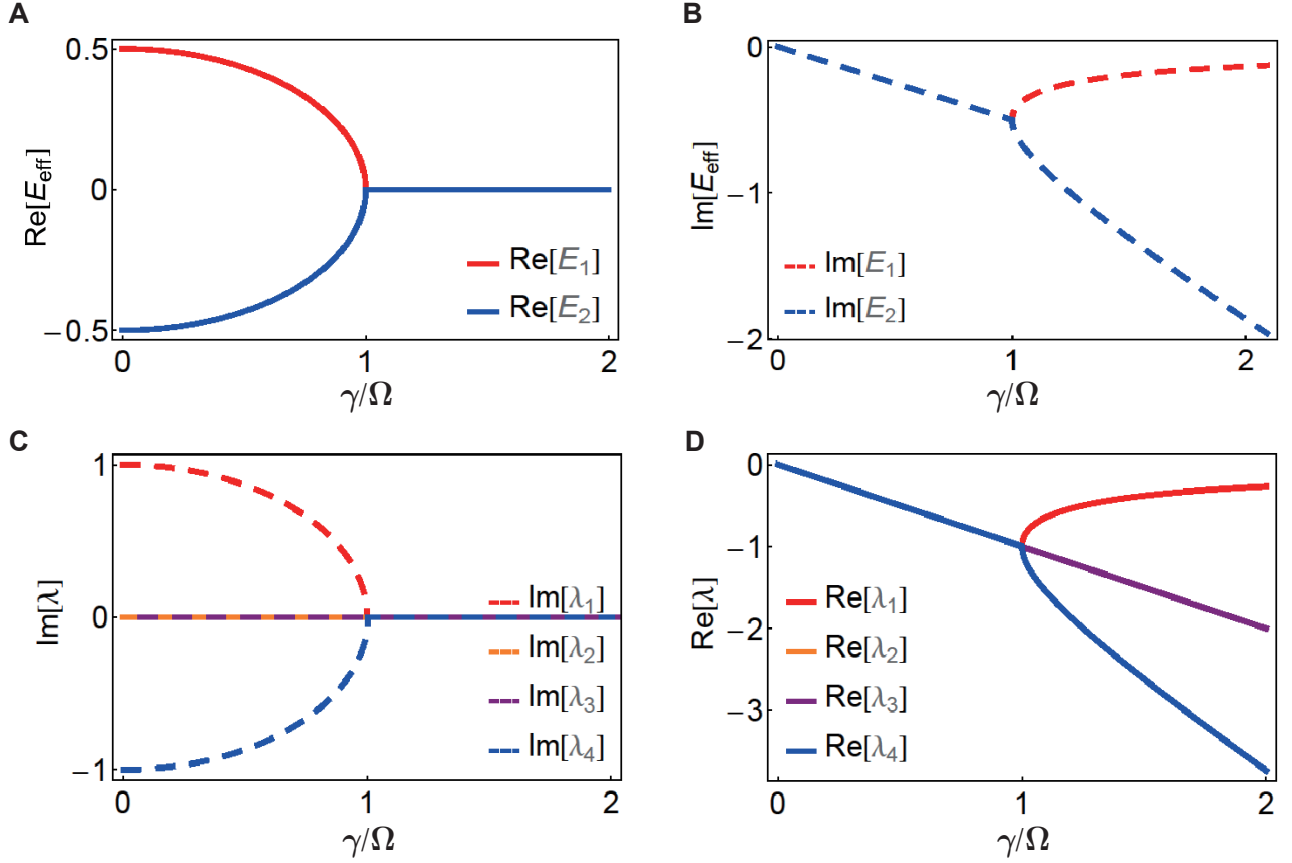


Figure S1: (A) The real parts of the eigenvalues of effective Hamiltonian. (B) The imaginary parts of the eigenvalues of effective Hamiltonian. (C) The imaginary parts of the eigenvalues of \mathcal{L} . (D) The real parts of the eigenvalues of \mathcal{L} . They show the same EP with $H_{\mathcal{PT}}$ as shown in Fig. 1(D).

At time t , the time evolution of the system from the initial state $\rho(0)$ is (except for the EP [1, 2]) $\rho(t) = \sum_{i=1}^4 e^{\lambda_i t} c_i R_i = e^{-\gamma t} \rho_{\mathcal{PT}}(t)$, where

$$\rho_{\mathcal{PT}}(t) = e^{\kappa t} c_1 R_1 + c_2 R_2 + c_3 R_3 + e^{-\kappa t} c_4 R_4 \quad (S7)$$

is the time evolution of \mathcal{PT} -symmetric system, $c_i = \text{Tr}[C_i \rho(0)]$ are coefficients of the initial state decomposition onto the eigenbasis of \mathcal{L} [2].

From this formula we can see that, when $\gamma > \Omega$, κ is real and bigger than zero so that the eigenmode R_1 dominates the dynamics finally with corresponding time evolution $e^{\kappa t}$. Therefore the \mathcal{PT} symmetry will increase exponentially. When $\gamma < \Omega$, the system is in a mixed state. The superposition of $\rho_{\mathcal{PT}}(t)$ has eigenmatrix R_1 and R_4 with corresponding time evolution $e^{\pm i|\lambda|t}$, which result in the oscillatory evolution at angular frequency $|\kappa|$.

$\rho_{\mathcal{PT}}$ in Eq. S7 tells us that the dynamics of the system behavior is totally different if we change the parameters γ/Ω . When $0 < \gamma < \Omega$, κ is an imaginary number, $\rho_{\mathcal{PT}}$ will oscillate periodically at frequency $|\kappa|$. When γ increase (but still smaller than Ω), the oscillating frequency will get smaller and smaller and till $\gamma = \Omega$, which is the EP, not only all the eigenvalues of \mathcal{L} is degenerated, but also the eigenvectors R_1 and R_4

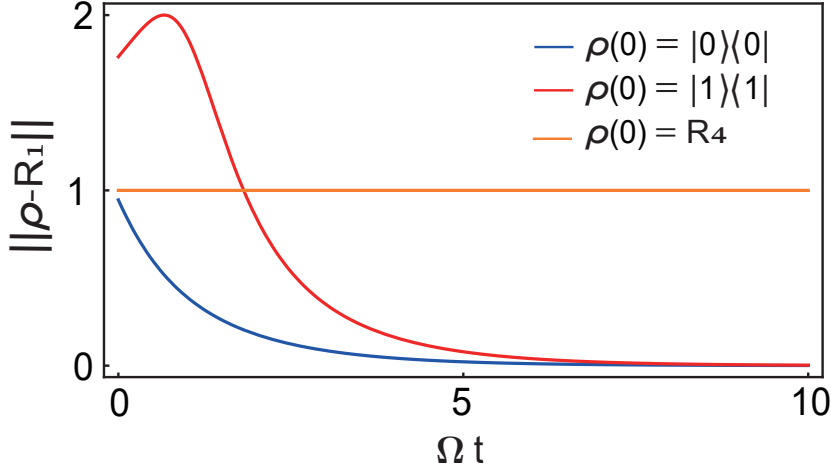


Figure S2: In PTB phase, the system will evolve to the ground state R_1 , whatever the initial state is, expect is the right eigenmatrix R_i . Because the right eigenmatrix R_i is the fix state of the system [4]. Here we set $\gamma/\Omega = 1.2$.

are degenerated, and

$$R_1(\gamma = \Omega) = \begin{pmatrix} 1 & -i \\ i & 1 \end{pmatrix}. \quad (\text{S8})$$

This means that at EP, the system will not oscillate any more, but be in the state R_1 , which is a maximum coherent superposition state. In the PTB phase, $\kappa > 0$, from equation of $\rho_{\mathcal{PT}}(t)$ we can see the time scale of the first eigenmode R_1 exponentially grows, which lead to the dynamics of the \mathcal{PT} system evolving exponentially. Meanwhile, when $\kappa t \gg 1$, $e^{-\kappa t} \rightarrow 0$ and the first mode R_1 dominates the dynamics of the system. That is to say the system of $\rho(t)$ will evolve to this stable state R_1 finally, whatever the initially state is. We characterize this in terms of the trace distance $||\rho(t) - R_1|| = \text{Tr}[\sqrt{(\rho(t) - R_1)^\dagger(\rho(t) - R_1)}]$ between $\rho(t)$ and R_1 for different initial state [2, 3]. The trace distance measures the distinguishability of two quantum states and the results are shown in Fig. S2. It shows that when the initial state is the eigenmodes of $\mathcal{L} R_i$, the state of the system will stay there, we call those states fixed points. This is because $\text{Tr}[C_{j \neq i} R_i] = 0$, so $\rho(t) = \rho(0) = R_i$. However, for other initial states, the system will evolve to the stable state R_1 finally.

If the initial state is $|0\rangle$, we can get the \mathcal{PT} density matrix at time t

$$\rho_{\mathcal{PT}}(t) = \begin{pmatrix} \frac{\Omega^2 \sinh(\kappa t/2)^2}{\kappa^2} & \frac{i \frac{\Omega(\gamma - \gamma \cosh(\kappa t) - \kappa \sinh(\kappa t))}{2\kappa}}{2\kappa} \\ -i \frac{\Omega(\gamma - \gamma \cosh(\kappa t) - \kappa \sinh(\kappa t))}{2\kappa} & \frac{-\Omega^2 + (2\gamma^2 - \Omega^2) \cosh(\kappa t) + 2\gamma\kappa \sinh(\kappa t)}{2\kappa^2} \end{pmatrix} \quad (\text{S9})$$

So

$$\langle \sigma_z^{\mathcal{PT}}(t) \rangle = -\cosh(\kappa t) - \frac{\gamma \sinh(\kappa t)}{k}, \quad (\text{S10})$$

$$\langle \sigma_y^{\mathcal{PT}}(t) \rangle = \text{Tr}[\sigma_y \rho_{\mathcal{PT}}] = \frac{\Omega}{\kappa^2}(-\gamma + \gamma \cosh(\kappa t) + \kappa \sinh(\kappa t)) \quad (\text{S11})$$

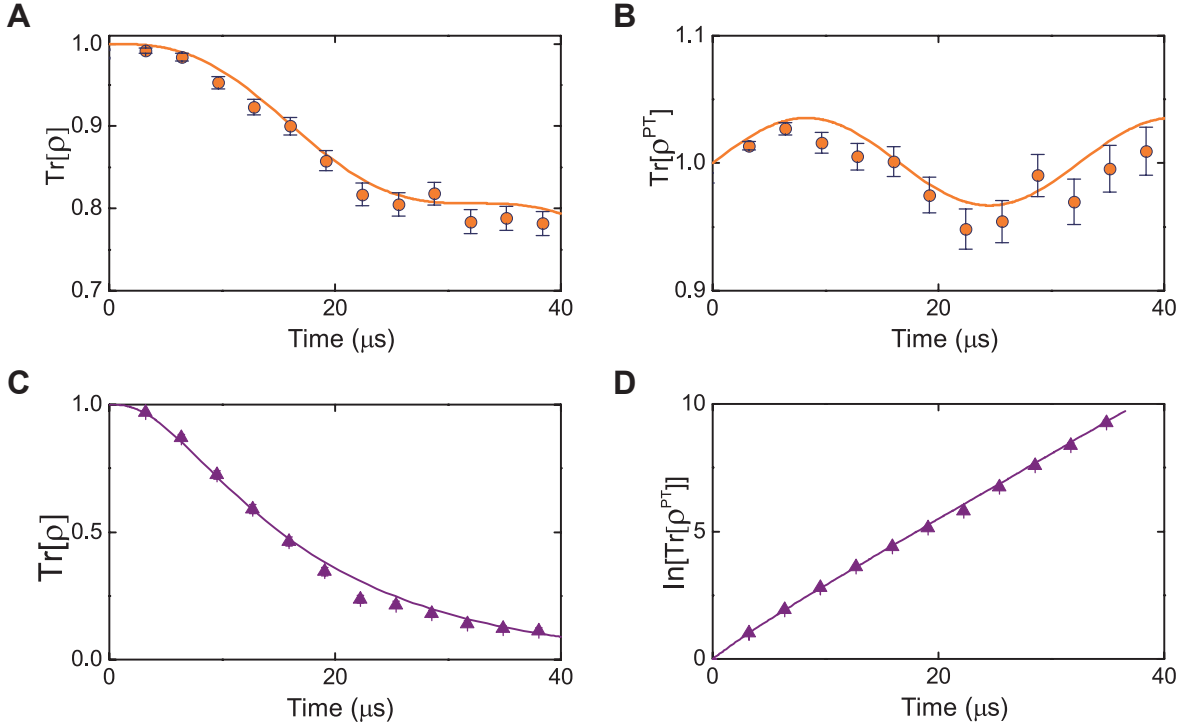


Figure S3: (Color online) (A-B) The trace of the density operator ρ (A) and $\rho_{\mathcal{PT}}$ (B) change with time in the PTS phase, with $\Omega = 2\pi \times 32$ (kHz), $\gamma = 2\pi \times 1$ (kHz). (C-D) The trace of the density operator ρ (C) and $\rho_{\mathcal{PT}}$ (D) change with time in the PTB phase, with $\Omega = 2\pi \times 32$ (kHz), $\gamma = 2\pi \times 47$ (kHz).

We have to mentioned that both $\rho(t)$ and $\rho_{\mathcal{PT}}(t)$, on their own, do not preserve the trace of the density operator (see Fig. S3). As shown in Fig. S3(A,C), for $\rho(t)$, which is a dissipative system, the trace is always decay whatever in PTS or PTB phase. But for $\rho_{\mathcal{PT}}(t)$, which has loss and gain, as shown in Fig. 3S(B,C), the trace will show \mathcal{PT} symmetry breaking phenomenon. So if we want to know the relative dynamics of the system, we need renormalize $\rho(t)$ by $\rho(t) = e^{\mathcal{L}t}\rho(0)/\text{Tr}[e^{\mathcal{L}t}\rho(0)]$ [3, 4], that is what we did in Eq. (4-5).

Appendix A.2. S2: Experiment realization of tunable loss rate γ

In our experimental scheme, the Zeeman sublevels ${}^2\text{S}_{1/2}(m_J = -1/2)$ and ${}^2\text{D}_{5/2}(m_J = +1/2)$ of the ${}^{40}\text{Ca}^+$ ion in a magnetic field of 5.2 G are chosen as system states $|0\rangle$ and $|1\rangle$, and the Zeeman sublevels ${}^2\text{S}_{1/2}(m_J = +1/2)$ is considered as an environment. ${}^2\text{D}_{5/2}(m_J = +1/2)$ is excited to ${}^2\text{P}_{3/2}(m_J = +3/2)$ by the circularly polarized 854 nm laser beam, and according to the selection rule, ${}^2\text{P}_{3/2}(m_J = +3/2)$ will only transit to ${}^2\text{S}_{1/2}(m_J = +1/2)$ by spontaneous radiation. Hence, the loss rate between the system and the environment can be realized by adjusting the intensity of 854 nm laser beam. Before we start the \mathcal{PT} experiment, the external state of the ${}^{40}\text{Ca}^+$ ion cooled to the

ground state by using Doppler cooling and sideband cooling, and the long life of ${}^2\text{D}_{5/2}$ guarantees that we don't have to worry about the spontaneous radiation from $|1\rangle$ to the $|0\rangle$ or $|2\rangle$ state. In this way we can obtain a Rabi oscillations of $|0\rangle$ without loss, which is the premise of accurate fitting of dissipation γ . The coupling Ω between state $|0\rangle$ and state $|1\rangle$ is obtained by fitting the experimental data of Rabi oscillation of $|0\rangle$, which is approximately equal to $2\pi \times 32$ (kHz) in all of our experimental settings. Finally, in order to realize \mathcal{PT} -symmetric system, the external state also should be cooled to the ground state, and both 854 nm and 729 nm laser beams were switched on at the same time. The quantum states of the ion at different times are read out by the electron shelving. Between different experiments, the intensity of 854 nm laser beam is controlled by modulating the acousmo-optic modulator (AOM). Therefore, we obtain the experimental data of dynamical evolution $\rho_{\mathcal{PT}}$ of the \mathcal{PT} -symmetric system for different intensities of 854 nm laser beam. According to $\rho(t) = e^{-\gamma t} \rho_{\mathcal{PT}}$, we can fit the loss rate γ corresponding to different intensities of 854 nm laser beam.

- [1] F. Minganti, A. Miranowicz, R. W. Chhajlany, F. Nori, Quantum exceptional points of non-Hermitian Hamiltonians and Liouvillians : The effects of quantum jumps. *Phys. Rev. A* **100**, 062131 (2019).
- [2] K. Macieszczak, I. Lesanovsky, J. P. Garrahan, Towards a Theory of Metastability in Open Quantum Dynamics. *Phys. Rev. Lett.* **116**, 240404 (2016).
- [3] K. Kawabata, Y. Ashida, M. Ueda, Information Retrieval and Criticality in Parity-Time-Symmetric Systems. *Phys. Rev. Lett.* **119**, 190401 (2017).
- [4] D. C. Brody, E. M. Graefe, Mixed-State Evolution in the Presence of Gain and Loss. *Phys. Rev. Lett.* **109**, 230405 (2012).